



Cellulose Nanocrystals Isolated from Bean Seed Hulls: Acetylation and Characterization

Ebele Joy Morah ^{a*}, David Okechukwu Okeke ^b,
Ozioma Juliana Anekwe-Nwekeaku ^a,
Chidinma Malinda Muobike ^a
and Uchechukwu Joachin Ezenyeaka ^a

^a Department of Pure and Industrial Chemistry, Nnamdi Azikiwe University, P.M.B 5025, Awka Anambra State, Nigeria.

^b Department of Applied Biochemistry, Nnamdi Azikiwe University, Awka, Nigeria.

Authors' contributions

This work was carried out in collaboration among all authors. All authors read and approved the final manuscript.

Article Information

DOI: 10.9734/AJACR/2023/v14i4276

Open Peer Review History:

This journal follows the Advanced Open Peer Review policy. Identity of the Reviewers, Editor(s) and additional Reviewers, peer review comments, different versions of the manuscript, comments of the editors, etc are available here: <https://www.sdiarticle5.com/review-history/111542>

Original Research Article

Received: 24/10/2023

Accepted: 29/12/2023

Published: 30/12/2023

ABSTRACT

Bean seed hulls is an agro-waste with abundant content of lignocellulosic materials but are being wasted due to its underutilization. Cellulose nanocrystals (CNCs) were successfully extracted from bean seed hulls using alkali treatment, bleaching and sulphuric acid hydrolysis. Cellulose triacetate (CTA) was obtained from CNCs by acetylation using acetic anhydride with sulphuric acid as catalyst. CNCs is neutral pH whereas CTA is slightly acidic. CNCs was sparingly soluble in ethanol but CTA was completely soluble in ethanol. CTA has a higher melting point than CNCs. The density of both CNCs and CTA is approximately equal to the density of water. SEM analysis revealed that CNCs is irregular and fragmented in nature and has both more large surface area and porosity than

*Corresponding author: Email: ej.morah@unizik.edu.ng;

CTA. FTIR analysis showed the presence of the dominant functional groups such as O-H stretch, N-H stretch, C-H stretch, C-O stretch and C-N stretch in both CNCs and CTA. GC-MS analysis revealed the presence of the prevalent organic compounds such as alkanes, alcohols, phenols, alkanones, phthalates, carboxylic acids, esters and triterpene in both CNCs and CTA. Therefore, the isolation of CNCs from bean seed hulls suggests great efficacy to recover the under-utilized agro-wastes thereby preventing air pollution.

Keywords: Bean seed hulls; Isolation; cellulose nanocrystals; cellulose triacetate; Characterization.

1. INTRODUCTION

The inability of most African countries to follow the universal trend of waste recycling has increased the quantity of agricultural trash produced yearly. Burning and open dumping of agro-wastes are prevalent practices in Nigeria. This burning of agro-wastes decreases agricultural output, contributes to climate change, contributes to unfriendly and undesirable environment and causes respiratory illness such as bronchitis, eye irritation, asthma etc. On the other hand, many of these agro-wastes are allowed to rot away unused. For instance, bean seed husks is a biomass that is carelessly dumped in different regions of Nigeria thereby resulting in environmental pollution [1-5]. The need to protect the environment from air pollution resulting from burning, open dumping or burying of agricultural wastes has led to the extraction of cellulose from these agro-wastes, which is economically and environmentally friendly. Thus, the trends of using agro-wastes and underused plants containing cellulosic fibres such as rice husks, rice straw, sugarcane bagasse, pineapple peels, bean seed husks, plantain stem, walnut shell, tomato peels, maize stem, maize cobs, corn fibres, cotton stalks, cotton seed hulls and burr, bamboo pulp, oil palm trees, saw dust from woods, raffia, wheat straw, wheat bran etc. are on the increase [6, 1, 7-10].

The demand for renewable and eco-friendly sustainable materials is ever-increasing and has tremendously increased the production of cellulose from agriculture biomass, marine animals, algae, protozoans, bacteria and fungi thereby making crop and animal wastes useful. Cellulose nanocrystals are referred to as second generation renewable resource. It also serve as a better replacement for the petroleum-based products. The major attention being given to nanocrystalline cellulose is on the increase because of its low density, great rigidity, great tensile strength, and high flexibility, renewable and biodegradable properties. Agricultural wastes biomass are of great importance because

of the following reasons: it is environmentally friendly, it has low cost, it is readily available, it is renewable and it exhibits acceptable mechanical properties [11-14, 9].

Lignin, hemicellulose and cellulose are the most important components of plants. Lignin covers, encloses and protects hemicellulose and cellulose. Hemicellulose is a polysaccharide composed of xylose, glucose, arabinose, mannose and galactose [15]. Cellulose is one of the most important polysaccharides produced in plants from carbon (iv) oxide and water by the process of photosynthesis and are made up of glucose units linked by a β - 1,4 -glycosidic linkage with a regular network of intra and intermolecular hydrogen bonds [16-19]. Cellulose with the formula $(C_6H_{10}O_5)_n$ is the chief structural material of plant cell walls which gives the plant rigidity and form. It is likely the most prevalent organic material known [1, 20, 21]. Acid hydrolysis using H_2SO_4 or HCl process is mainly used for the isolation of cellulose nanocrystals (CNCs) from cellulose fibres present in different vegetable natural sources. Sulphuric acid hydrolysis introduces small number of sulphate ester groups into the surface of the CNCs making it easily dispersed in water whereas HCl hydrolysis leaves the surface chemistry of CNCs unchanged. Cellulose nanocrystals have been generally considered as reinforcement segment in biodegradable plastic because of their biodegradability, easy accessibility, very crystalline form and capacity to enhance the qualities of bio composite [22, 23, 16, 24, 25]. Cellulose is the starting material for the production of cellulose triacetate. When the cellulose is treated with acetic anhydride or acetic acid in the presence of sulphuric acid, cellulose triacetate can be formed [20]. The high resolution image of cellulose triacetate is represented in Fig. 1b [26].

Squalene, a triterpene present in CNCs has anti-cancer activity especially the tumour growth around blood vessels [27]. Amines are used as painkillers, as anaesthetic, as solvents in

Benadryl syrups, regulates vitamin levels in the body and serves as useful stimulants for neurotransmitters like serotonin for our bodies [28]. Carboxylic acids are used as solubilizer for antibiotic or antihistamine drug, as antihypertensive drugs, as blood cholesterol reducing drugs, as nonsteroidal anti-inflammatory drugs and as analgesics [29, 30]. Thiol containing drugs are used as chelators of heavy metal ions, removing them from blocking enzyme activity in the body and promoting oxidation; they serve as antioxidants in the body i.e prevents the oxidation of protein, lipids and DNA in the body [31]. Ketones are used in chemical peeling and for acne treatments; ketones maintain brain function in the absence of glucose; enter the bloodstream and are used by the heart, kidney and skeletal muscle [32]. Phenols act as antioxidants and prevents cancer but can be toxic in high amounts; relieves symptoms caused by sore throat, used as preservatives in vaccines; phenol-based products are used as oral analgesics; used to treat tight muscles [33]. Phenolic compounds exhibits various biological activities such as antimicrobial, anti-inflammatory and antioxidant properties [34,35]. Dihydroxy isosteviol methylester with the highest percentage composition of 26.58% is capable of inducing apoptosis in cancer cells signifying its utilization in drug design for chemoprevention [36]. Phthalates are converted to metabolites in the body which is excreted in urine, faeces and sweats. In human, phthalates cause type II diabetes, insulin resistance, overweight /obesity, allergy, asthma, higher systolic blood pressure, low birth weight, earlier menopause, pregnancy loss, preterm birth. Some phthalate metabolites were negatively associated with breast cancer, increased risk of thyroid cancer in children,

toxicity on genetal development; determines semen quality and precocious puberty in male children [37]. Steroids are anti-inflammatory drug used to treat rheumatoid arthritis, lupus or vasculitis (inflammation of the blood vessels) [38]. Halogenated aliphatic and aromatic hydrocarbons are known to exhibit high activity against different nematodes and trematodes parasitizing domestic animals and humans [39]. Fatty acids are used as a vehicle and lubricant in pharmaceutical preparations; it have been used extensively as an additive for development of nanodrug delivery systems [40]. Aliphatic hydrocarbons are used in extraction processes in pharmaceuticals; they are axphysiants and central nervous system depressants. Many paraffins cause chemical pneumonitis [41]. Aliphatic and aromatic alcohols are used as antiseptic, disinfectant and antidote; used as a solvent and intermediate in the pharmaceutical industries; used in human medicine as an anti-microbial preservative and as a local anesthetic and antipruritic. Aliphatic alcohols show increasing potency as non-selective central nervous system depressants [42]. Conjugated dienes demonstrates antifungal and antibacterial properties [43, 44].

The aims of this study are to (i) isolate raw cellulose from bean seed husks and then convert it to CNCs (ii) convert the CNCs to cellulose triacetate (iii) determine some of the physical properties of both CNCs and CTA (iv) investigate the chemical characterization of both CNCs and CTA using Scanning electron microscopy (SEM), Fourier transform infrared (FTIR) and Gas chromatography-mass spectrometry (GC-MS) analyses (v) ascertain the effect of acetylation on the physico-chemical properties of CNCs.

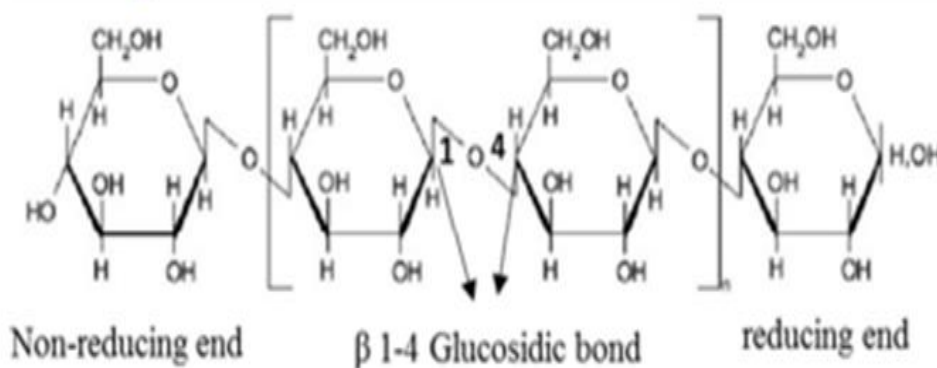


Fig. 1a. Structural image of cellulose

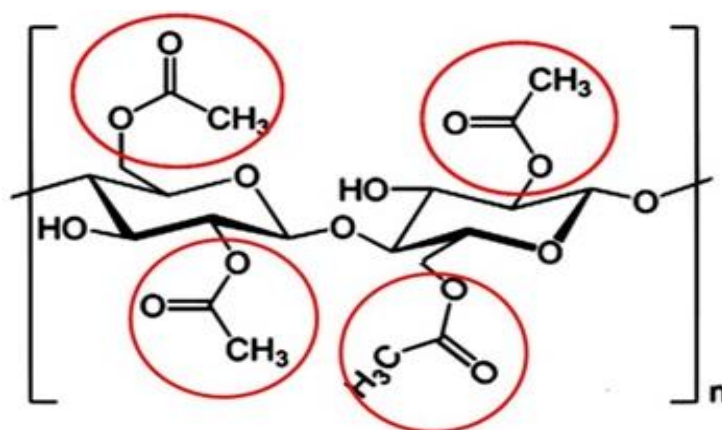


Fig. 1b. High resolution image of cellulose triacetate

2. MATERIALS AND METHODOLOGY

2.1 Collection and Processing of Sample

The beans hulls were gotten from Ubani main market in Umuahia North Local Government Area of Abia State, Nigeria and then ground with a grinding machine into fine particles and became ready for cellulose extraction.

2.2 Materials

Conical flask, Weighing balance, Beaker, Oven, Masking Tape, Filter Paper, Foil, Measuring Cylinder, Spatula, Magnetic stirred heater, Crucible, pH meter, Pipette, glass centrifuge tubes, gooch crucible, Buck Scientific M530 USA FTIR, SEM Quanta FEG450(FEI)(APOLLOX-EDAX), Buck M910 Gas Chromatograph equipped with HP-5MS Column, shaking water bath, mechanical stirrer, test tubes, universal indicator, dropper, glass stirring rod, dessicator, Erlenmeyer flask, reflux condenser, petri dish, platinum crucible, muffle furnace, pycrometer, melting point apparatus.

2.3 Reagents

Ether, Ethanol, Distilled water, Sodium hydroxide (NaOH), Sulphuric acid (H₂SO₄), Sodium hypochlorite (NaOCl), Acetic anhydride, glacial acetic acid, 2-naphtol, Schweitzer's reagent, Conc. HCl, deionized water, conc. Nitric acid, nujol, benzene, potassium bromide (KBr), deuterated triglycerine sulphate.

2.4 Methods

2.4.1 Alkali treatment

Exactly 5 grammes of the ground sample of bean hulls was dissolved in 2 w/v% NaOH in a solid to

liquid ratio of 1 g/10 ml. The solution was then heated at 40°C for 45 mins in a shaking water bath for 4hours. The alkali treatment was repeated 4 times until no more discoloration occurred. The sample solution was further washed with distilled water until pH 7 (neutral) was obtained and then the sample was oven dried at 60°C until a constant weight was obtained. The cellulose was hydrolysed with 2 w/v% NaOH for 15 mins, 30 mins and 45 mins respectively at 40°C [6].

2.4.2 Bleaching treatment

The essence of bleaching process is to remove lignin and other components so as to obtain purified cellulose. The sample resulting from the alkali treatment is blended with the bleaching agent sodium hypochlorite. 1g of sample to 50ml of bleaching agent solution is heated at 80°C, shaken at 100 rpm for 2 hours using a shaking water bath and repeated two times to obtain a white product. The bleached sample was then thoroughly washed using distilled water until pH 7 to obtain white cellulose [6].

2.4.3 Sulphuric acid hydrolysis

Cellulose nanocrystals were then isolated from the white cellulose by acid hydrolysis through the treatment with 64 w/w% sulfuric acid solution at 50°C for 30 mins, 60 mins and 90 mins respectively under constant mechanical stirring. This suspension was diluted 10-fold with cold deionized water to quench the hydrolysis reaction and then centrifuged to remove the excess acid. The resultant precipitate was washed several times by centrifugation with deionized water until a neutral pH was reached finally yielding the cellulose nanocrystals [45, 46].

2.4.4 Confirmatory test for cellulose

The best reagent for confirming cellulose is Schweitzer's reagent. CNCs was treated with the Schweizer's reagent (tetraammine copper (ii) hydroxide dihydrate). Cellulose was also treated with conc. HCl. Schweitzer's reagent is a deep blue solution prepared by dissolving copper (ii) hydroxide in excess of ammonia. It has a strong ammonia smell.

2.4.5 General test for carbohydrate

Molisch's Test: This is a general test for carbohydrates. 5mg of the cellulose nanocrystals was placed in a test tube containing 0.5 ml of water and mixed with 2 drops of 10% solution of 2-naphtol in ethanol. 1 ml of conc. sulphuric acid was pipetted into the solution, the acid formed a layer beneath the aqueous solution common surface of the liquids; the colour quickly changed on standing or shaking with a dark purple solution being formed. The mixture was shaken and allowed to stand for 2 minutes. A dull violet precipitate appeared [47].

$$\% \text{ Cellulose} = \frac{\text{mass of CNC obtained}}{\text{mass of initial sample}} \times \frac{100}{1}$$

2.4.6 Acetylation of cellulose nanocrystals

Acetylation of cellulose nanocrystals using acetic anhydride or acetic acid in the presence of the catalyst H₂SO₄ gives the textile material named Cellulose triacetate. The three -OH groups of the cellulose were acetylated.

Procedure: About 5 g of the CNCs was dissolved in 10ml of glacial acetic acid and heated at 47.5°C for 1 hour and 5 ml of acetic anhydride added with 5.5 wt% sulfuric acid as catalyst. The mixture was further heated for 3hours at the same temperature. After the completion of acetylation process, the acetylated cellulose was thoroughly washed to remove odour and any possible soluble impurities that may have accompanied the reaction process and it is then dried in an oven at 60°C to constant weight [10].

$$\text{Weight percent gain (WPG)} = \frac{W_{\text{final}} - W_{\text{initial}}}{W_{\text{initial}}} \times \frac{100}{1}$$

Where,

W_{final} = weight of oven dried acetylated CNC
 W_{initial} = weight of CNC before acetylation

2.4.7 Procedure for solubility tests

a) Solubility in water

Exactly 0.10 g portion of the cellulose nanocrystals or cellulose triacetate in a small test tube (100 x 12mm) was treated with successive 1.0 ml portion of H₂O shaking vigorously after each addition, until 3.0ml was added. If the cellulose does not dissolve completely in 3.0 ml of H₂O, it may be regarded as insoluble in water. The content of the small test tube was tested with universal indicator paper, a little of the solution or supernatant liquid was removed with a dropper [47].

b) Solubility in ether

About 0.10 g of the solid cellulose nanocrystals or cellulose triacetate in a dry small test tube was treated with successive 1.0 ml portions of ether, shaking vigorously after each addition, until 3.0 ml of ether was added. More than 3 ml of ether shouldn't be employed [47].

c) Solubility in ethanol

0.10 g of the solid cellulose nanocrystals or cellulose triacetate in a dry small test tube was reacted with successive 1.0 ml portions of ethanol shaking vigorously after each addition until 3.0 ml of ethanol was completely added [47].

2.4.8 Determination of cellulose content

Raw cellulose content was measured according to **ASTM, 2017**. 0.3 g of sample was weighed into 50 ml glass centrifuge tubes containing 50 ml of water, centrifuged at 1500 rpm for 10 mins, and the supernatant decanted. The sample was resuspended in 12.5 ml glacial acetic and 2.5 ml of concentrated nitric acid and digested in a boiling water bath for 20 min and the supernatant collected. The supernatant was transferred to a Gooch crucible (W_1), washed successfully with hot alcohol, 10 ml of 90% benzene, and 60% of ether, dried and weighed, (W_3) finally ashed (W_2) and reweighed [48].

$$\text{Cellulose content} = \frac{W_3 - W_2}{W_1} \times 100$$

W_3 = weight of dried sample

W_2 = weight of ash content

W_1 = weight of sample

2.4.9 Lignin content determination

0.3 ± 0.01 g prepared sample was weighed to the nearest 0.1 mg and placed in a 16 x 100 mm test tube. The initial sample weight was recorded

as W_1 . Each sample was run in duplicate, at minimum. Samples for total solids determination (LAP-001) were weighed out at the same time as the sample for the acid – insoluble lignin determination. If this is done later, it can introduce an error in the calculation because ground biomass can rapidly gain or loss moisture when exposed to the atmosphere. The average total solids values were recorded as T_{final} . 3.00 ± 0.01 ml (4.92 ± 0.01 g) of 72% H_2SO_4 was added and a glass stirring rod used to mix for 1 minutes, or until the sample is thoroughly wetted. The test tube was placed in the water bath controlled to $30 \pm 1^\circ C$ and hydrolyzed for 2 hours and then cooled in a desiccator and the weight, W_2 i.e the weights of the crucible, acid–insoluble lignin, and acid–insoluble ash were recorded to the nearest 0.1mg [48].

Calculation % acid – insoluble residue on an extractives – free basis as follows:

$$\% \text{ acid – insoluble residue} = \frac{W_2 - W_3}{W_1 \times \% \frac{T_{final}}{100\%}} \times 100\%$$

Where

W_1 = initial weight of extracted sample

W_2 = weight of crucible, acid-insoluble residue, acid–insoluble ash

W_3 = weight of crucible and acid- insoluble ash

$\% T_{final}$ = % total solids of the extracted sample determined at $105^\circ C$ as described by the standard method for the determination of total solids in biomass.

2.4.10 Hemicellulose determination

Hemicelluloses content was measured according to ASTM, 2017. 1g of sample was weighed and placed in a 20 x 150 mm test tube and recorded as W_1 , the initial sample weight. 15ml of 72% was added and stirred for 1minute until the sample was thoroughly wetted. The sample was transferred to a 1000ml Erlenmeyer flask and diluted to 500 ml with deionized water. The flask was then placed on the heating manifold and attached to the reflux condenser, gently boiled and refluxed for 4 hours. At the end of 4 hours, the condenser was rinsed with a small amount of deionized water before disassembling reflux apparatus. The hydrolyzed solution was placed on the crucibles. The weight of collected filtrate was measured. The crucible and contents was

dried at $105 \pm 30^\circ C$ for 2 hours and then cooled in dessicators and recorded as W_2 . The weight of the crucible, and contents were placed in the muffle furnace and ignited at $575^\circ C$ for a minimum of 3 hours, or until all the carbon is eliminated. Then it was cooled in dessicators and recorded as W_3 [48].

Note: Total solid = 100 – moisture content

Calculations

$$\% \text{ Hemicellulose} = \frac{W_2 - W_3}{W_1 \times \% \frac{T_{final}}{100\%}} \times 100\%$$

Where W_1 = initial sample weight.

W_2 = weight of crucible and dried content

W_3 = weight of crucible and contents minus carbon

2.4.11 Moisture content determination

A petri-dish was washed and dried in the oven. Approximately 1-2 g of the sample was weighed into petri dish. The weight of the petri dish and sample was noted before drying. The petridish and sample were put in the oven and heated at $105^\circ C$ for 2 hr with the result noted and heated another 1 hr until a steady result was obtained and the weight was noted. The drying procedure was continued until a constant weight was obtained [48].

$$\% \text{ Moisture content} = \frac{W_1 - W_2}{\text{Weight of sample}} \times 100$$

Where W_1 = weight of petridish and sample before drying

W_2 = weight of petridish and sample after drying.

2.4.12 Ash content determination

AOAC, 2017 method was used. Empty platinum crucible was washed, dried and the weight was noted. Approximately 1- 2 g of sample was weighed into the platinum crucible and placed in a muffle furnace at $550^\circ C$ for 3 hours. The sample was cooled in a dessicator after burning and weighed [49].

Calculations:

$$\% \text{ Ash content} = \frac{W_3 - W_1}{W_2 - W_1} \times 100$$

Where

W_1 = weight of empty platinum crucible

W_2 = weight of platinum crucible and sample before burning

W_3 = weight of platinum and ash.

2.4.13 Direct pH determination

A small quantity of the sample was dissolved in water or another solvent, and the pH of the resulting solution was measured using a pH meter [50].

2.4.14 Density determination

Pycnometer method: A small, calibrated glass container (pycnometer) was filled with a known volume of liquid and weighed. The pycnometer was then emptied and filled with the sample, and the weight measured again. The difference in weight between the two measurements was used to calculate the volume of the sample, which was then used to determine the density [48].

2.4.15 Melting point determination

The capillary tube containing the sample was inserted into a slot behind the viewfinder of a melting point apparatus. There are usually three slots in each apparatus, and multiple melting points was taken simultaneously. The apparatus was turned on and the setting adjusted to an appropriate heating rate. The rate of heating is often experimental and was adjusted by careful monitoring of the thermometer on the apparatus. A magnified view of the illuminated sample in the apparatus was seen by looking through the viewfinder. The sample was heated at a medium rate to 20°C below the expected melting point, then the rate of heating slowed such that the temperature increases by not more than 1°C every 30 seconds (i.e., very slowly). The process was repeated with a fresh sample after allowing the apparatus to cool and the recommendations for compound with known expected melting point was used to perform a more careful assessment of the melting point [48].

2.5 Instrumental Analysis

2.5.1 Procedure for FTIR

Buck scientific M530 USA FTIR was used for the analysis. This instrument was equipped with a detector of deuterated triglycine sulphate and beam splitter of potassium bromide. The

software of the Gram A1 was used to obtain the spectra and to manipulate them. An approximately of 1.0 g of samples, 0.5 ml of nujol was added, they were mixed properly and placed on the salt pellet. During measurement, FTIR spectra was obtained at frequency regions of 4,000– 600 cm^{-1} and co-added at 32 scans and at 4 cm^{-1} resolution. FTIR spectra were displayed as transmitter values.

2.5.2 Scanning electron microscope

Morphological investigations of the composite particles were carried out with SEM Quanta FEG 450 (FEI) (APOLLO X - EDAX), U.S.A. 0.5 g Samples were coated with Au/Pd film and the SEM images were obtained using a secondary electron detector. Point chemical analysis was performed in 2 independently selected particles.

2.5.3 Quantification by GC-MS

The analysis of phytochemical was performed on a BUCK M910 U.S.A Gas chromatography equipped with HP-5MS column (30 m in length x 250 μm in diameter x 0.25 μm in thickness of film). Spectroscopic detection by GC–MS involved an electron ionization system which utilized high energy electrons (70 eV). Pure helium gas (99.995%) was used as the carrier gas with flow rate of 1 ml/min. The initial temperature was set at 50–150 °C with increasing rate of 3 °C/min and holding time of about 10 min. Finally, the temperature was increased to 300 °C at 10 °C/min. One microliter of the prepared 1% of the extracts diluted with respective solvents was injected in a splitless mode. Relative quantity of the chemical compounds present in each of the extracts of was expressed as percentage based on peak area produced in the chromatogram.

2.6 Statistical Analysis

The physical characterization were carried out in duplicates, and then the mean determined followed by subjection to standard deviation using Microsoft excel 2010 package. The weight percent gain plots were done using the statistical software named Origin Pro graphing and analysis 2021.

3. RESULTS AND DISCUSSION

3.1 Physical Properties

Cellulose nanocrystals dissolved in both schweitzer's reagent and conc. HCl confirming its

presence. CNCs gave a positive test for carbohydrate. Table 1 shows the data for the solubility test of CNCs and CTA in the solvents such as ethanol, water and ether. It is observed that cellulose nanocrystals is sparingly soluble in ethanol while the acetylated cellulose nanocrystals is completely soluble in ethanol. Cellulose is quite polar. CNCs is sparingly soluble in both water and ether, although it contains a large number of hydroxyl groups. This is because cellulose is a large molecule held together by covalent bonds, hydrogen bonds and Vander Waals forces which are difficult to break. CTA is moderately polar and is sparingly soluble in water because it does not have a similar structure with water. Both CNCs and CTA are insoluble in ethanol because ethanol has low hydroxyl content [51, 47]. Out of the three solvents, ether was the best which dissolved both CNCs and CTA. From Table 2, the chemical content of the raw ground bean seed hulls were in the order cellulose (27.333%) > lignin (10.918%) > hemicellulose (6.034%) > ash content (8.170%) indicating that cellulose is the main component of plant cell walls which gives plant rigidity and form. From Table 3, CTA has a higher melting point (228.31°C) than cellulose nanocrystals (142.50°C). The density of CNCs (1.1005g/ml) is slightly higher than that of CTA (0.90 g/ml). Both the densities of CNCs and CTA are approximately equal to the density of water (1.00g/ml) indicating that the particles of CNCs and CTA will form suspensions in water. The pH of CNCs is neutral (7.00) indicating that $[H^+] = [OH^-]$ whereas the pH of CTA is very slightly acidic (6.59) showing that $[H^+] > [OH^-]$ [52]. CNCs gave an extremely higher yield (42.31%) than CTA (3.28%). The moisture content in both CNCs (6.35%) and CTA (2.90%) were very low showing that it will be difficult for micro-organisms to break them down and therefore they could be stored for a long time without adding preservatives [53,54].

3.2 Morphological Analysis

The microscopic morphology of samples was observed using SEM. The SEM image of CNCs were observed under magnifications of 300x, 500x, 750x and 1000x respectively at a voltage of 15 kV (Fig.2). CNCs exhibited a rough surface and irregular fragments with disordered large surface area. The pores were well developed indicating that CNCs can serve as a good adsorbent [55, 56]. Acetylation greatly influenced the morphology of CNCs. The SEM micrograph of CTA was taken at the voltage of 10 kV under

magnifications of 300x, 500x, 1000x and 1500x respectively as depicted in Fig.3. The amount of the fragments and pore sizes in CTA were greatly reduced with very small surface area. As a result, CTA will not be an effective adsorbent when compared to CNCs [57, 58]. There was reconfiguration of the disordered fragments into a very few ordered particles in CTA. The interfacial space among the fragmented particles were very narrow in CNCs but extremely wide in CTA. From the scanned image, the pore sizes of the fragmented particles in both CNCs and CTA decreased with increasing magnification. The porosity of CNCs were greatly higher than that of CTA making it a better adsorbent than CTA [59, 60].

3.3 FTIR Analysis

The structures of CNCs and CTA samples were analysed using FTIR (Fig. 4a & 4b). The bands observed in both spectra are strongly associated with the structures of cellulose, cellulose triacetate, hemicellulose, pectin, wax and lignin, suggesting that lignin and hemicellulose contents in the sample were not completely removed by the pre-treatment process.

Considering Fig. 4, Table 4 and Table 5, methyl and methylene groups both have asymmetric and symmetric C-H stretching vibration modes, giving rise to four absorption bands just below 3000 cm^{-1} . The presence of a small sharp band just above 3000 cm^{-1} is due to unsaturated $=\text{C-H}$ stretching vibration of alkenes. The in-plane bending vibration (or scissoring) of the C-H bond in $=\text{CH}_2$ group produces a band near 1415 cm^{-1} . The adsorption in the $1420\text{-}1290\text{ cm}^{-1}$ region with weak intensity is as a result of in-plane bending of the unsaturated C-H bond. The C=C stretching vibration gives rise to an absorption band in the $1680\text{-}1620\text{ cm}^{-1}$ region in simple alkenes; the band is of variable intensity but is much less intense than that from the C=O stretching vibration which also leads to absorption in this region. Conjugated double bonds of aliphatic systems such as dienes, trienes and tetraenes show two, three and four bands respectively in the $1650\text{-}1600\text{ cm}^{-1}$ region [47]. The $\text{C}\equiv\text{C}$ stretching vibration gives rise to a weak absorption in the $2260\text{-}2100\text{ cm}^{-1}$ region of the spectrum with variable intensity [47, 61]. Free O-H stretching band for alcohols and phenols is in the $3650\text{-}3590\text{ cm}^{-1}$ region. O-H band recognised as strong broad band in the $3400\text{-}3200\text{ cm}^{-1}$ region is due to intermolecular hydrogen bonding which results in the weakening of the O-H bond;

thus, broadening and shifting to lower frequency. Hydrogen bonded O-H of carboxylic acids show absorption in the region 3300-2500 cm^{-1} with very broad band [52, 47, 61]. The band at 1060 cm^{-1} is characteristics of C-O stretch for primary alcohols. The C-O stretching vibrations in esters give rise to very strong bands in 1300-1100 cm^{-1} [47, 52]. Allenes show a moderately intense band (sometimes as a double peak) at 2000- 1900 cm^{-1} due to the asymmetric C=C=C stretching vibrations [47, 61]. In dilute solutions, primary amines give two absorption bands, one near 3500 cm^{-1} and the other near 3400 cm^{-1} arising from the asymmetric and symmetric stretching vibrations of the two N-H bonds. The N-H out of plane bending of amines within the absorption range of 910-660 cm^{-1} [47, 61, 52]. All acid anhydrides show two strong absorption bands of C=O stretch near 1800 cm^{-1} and 1750 cm^{-1} , and they are almost always 60 cm^{-1} apart [47, 61]. C-O stretch and O-H in-plane deformation vibrations of carboxyl groups absorb at 1440-1395 cm^{-1} (weak). The C-O stretching vibration in esters give rise to very strong bands in 1300-1100 cm^{-1} region [47, 61]. C=O stretch of tertiary amide in dilute solution absorb at 1670-1630 cm^{-1} region with strong band [52]. C-N stretch of aromatic amine absorption band falls in the range 1340-1260 cm^{-1} [52]. The in-phase, out-of-plane, wagging vibrations of adjacent hydrogens of substituted benzenes give rise to strong absorption in well-defined frequency ranges in the 900-690 cm^{-1} region of the spectrum [47, 61]. The adsorption pattern with meta-substituted benzenes give rise to two apparent bands, one at 810-750 cm^{-1} and the other at 900-860 cm^{-1} [47, 61]. S=O stretch of sulphur compounds absorbs in the region of 1060-1040 cm^{-1} with strong band [47, 61]. Inorganic ions such as cyanide, thiocyanate and cyanate absorb in the region of 2200-2000 cm^{-1} [61].

3.4 GC-MS Analysis

Gas chromatography mass spectrometry is used to determine the chemical composition of the CNC and its derivative cellulose triacetate. The

GC-MS results of cellulose nanocrystals (Fig. 5 and Table 6) revealed the presence of organic compounds such as aliphatic hydrocarbons, phenolic compounds, saturated aliphatic carboxylic acids, aliphatic halogenocarboxylic acid, unsaturated aliphatic hydrocarbons, aliphatic ketones, aromatic ketone, diene, phthalate esters, aromatic alcohol, thiol, fatty acids, unsaturated aliphatic carboxylic acid, alkane sulphonyl chloride, triterpene, steroid, esters, aromatic alcohol, organometalloid compounds and amine [47]. On the other hand, the GC-MS results of cellulose triacetate (Fig.6 and Table 7) disclosed the presence of organic compounds such as saturated aliphatic hydrocarbons, unsaturated aliphatic hydrocarbons, aliphatic alcohols, saturated halogeno aliphatic compound, aliphatic ketone, phthalate esters, aliphatic carboxylic acid, aliphatic halogenocarboxylic acid, esters and triterpene [47].

Table 1. Solubility Data

Compound	Solvent		
	Water	Ethanol	Ether
CNCs	Sparingly soluble	Insoluble	Sparingly soluble
CTA	Sparingly soluble	Insoluble	Completely soluble

Solubility test was run five times for each compound

Table 2. Chemical composition of raw bean seed hulls

Component	% Yield
Hemicellulose	6.034
Ash content	8.170
Lignin	10.918
Cellulose	27.333

3.5 Weight Percent Gain (WPG)

Fig. 7, 8, and 9 show the plots of WPG over reaction time, catalyst concentration and temperature of the acetylation of CNCs. In Fig.7, the WPG of acetylated cellulose

Table 3. Physical characterization of CNCs and CTA from bean seed hulls

Parameter	CNCs	CTA
% Yield	42.31 ± 0.156	3.28 ± 0.106
% Moisture	6.35 ± 0.212	2.90 ± 0.940
pH	7.00 ± 0.141	6.59 ± 0.014
Density (g/ml)	1.1005 ± 0.002	0.90 ± 0.003
Melting point (°C)	142.50 ± 3.536	228.31 ± 0.014

Data reported as mean of duplicate determinations ± standard deviation

Table 4. FTIR spectra results for CNCs extracted bean seed hulls

Frequency (cm ⁻¹)	Functional group
882.948	N-H out-of-plane bend of amines In-plane, out-of-plane wagging vibrations of adjacent hydrogens of meta-substituted benzenes
1395.274	C-O stretch of esters, carboxylic acids O-H bend of alcohols
1628.171	C=C of non-conjugated alkenes C=O stretch of tertiary amide
1955.458	C=C=C Stretch of allenes
2180.658	[O-C≡N] ⁻ of cyanates, C≡N ⁻ of cyanides, [SC≡N] ⁻ of thiocyanates C≡C stretch of alkynes
2644.442	Hydrogen-bonded O-H stretch of carboxylic acids
2921.153	Hydrogen bonded O-H stretch of carboxylic acids C-H stretch of alkanes
3182.692	Intra-molecular H-bonded O-H of alcohols N-H stretch of primary amide
3381.938	N-H stretch of primary aromatic amine N-H stretch of primary amide
3601.981	Free O-H stretch of alcohols and phenols
3686.06	Free O-H stretch of alcohols and phenols

Table 5. FTIR spectral results for cellulose triacetate

Frequency (cm ⁻¹)	Functional group
1059.671	C-O stretch of alcohols S=O stretch of sulphur compounds
1290.03	C-N stretch of aromatic amines C=O stretch for esters
1415.428	O-H in-plane bend of carboxylic acids In-plane bending of unsaturated C-H bond of =CH ²
1627.85	N-H in plane bend of primary amine C=C stretch of alkenes Free C=O stretch of tertiary amide
1873.115	C=O stretch of acid anhydride
2165.219	[O-C≡N] ⁻ of cyanates, C≡N ⁻ of cyanides, [SC≡N] ⁻ of thiocyanates C≡C stretch of alkynes
2548.496	Hydrogen bonded O-H of carboxylic acids
2662.726	Hydrogen bonded O-H of carboxylic acids
2863.589	C-H stretch of alkanes
2977.214	C-H stretch alkanes Intra-molecular H-bonded O-H of alcohols in chelate form
3092.581	=C-H of alkenes
3207.265	Hydrogen bonded O-H of alcohols
3395.579	N-H stretch of primary aromatic amine
3499.734	N-H stretch of primary aliphatic amine
3584.56	Free O-H stretch of alcohols and phenols
3882.972	Free O-H stretch of alcohols and phenols

fluctuated with reaction time increment as well as with the fluctuation of catalyst concentration. In Fig. 8, the temperature of acetylation fluctuated alongside with the fluctuation of WPG. WPG of

acetylated cellulose decreased at constant temperature of 47.5°C. Table 8 displayed that the WPG was least (29.87%) at the highest temperature (60°C) but highest (72.22%) at mid

temperature of 47.50°C. In Fig. 9, WPG decreased at constant concentration of catalyst of (5.50 wt%). The WPG of acetylated cellulose decreased both at constant catalyst concentration of 5.50 wt% and at constant

temperature of 47.5°C. The reduction in WPG with increase in temperature was as a result of degradation of carbohydrate cellulose under the condition of strong acid and high temperature [10, 62, 63].

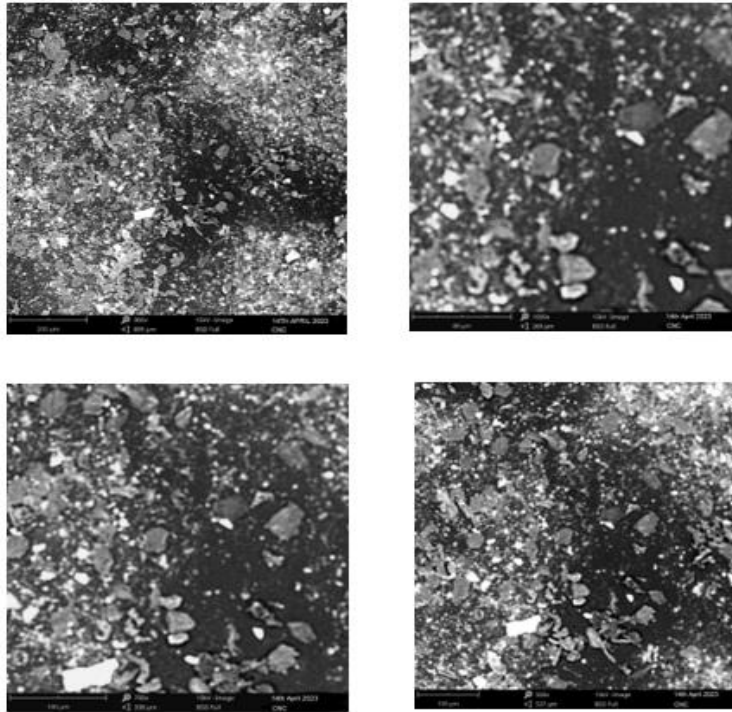


Fig. 2. SEM images of cellulose nanocrystals from alkali treated and bleached bean seed hulls

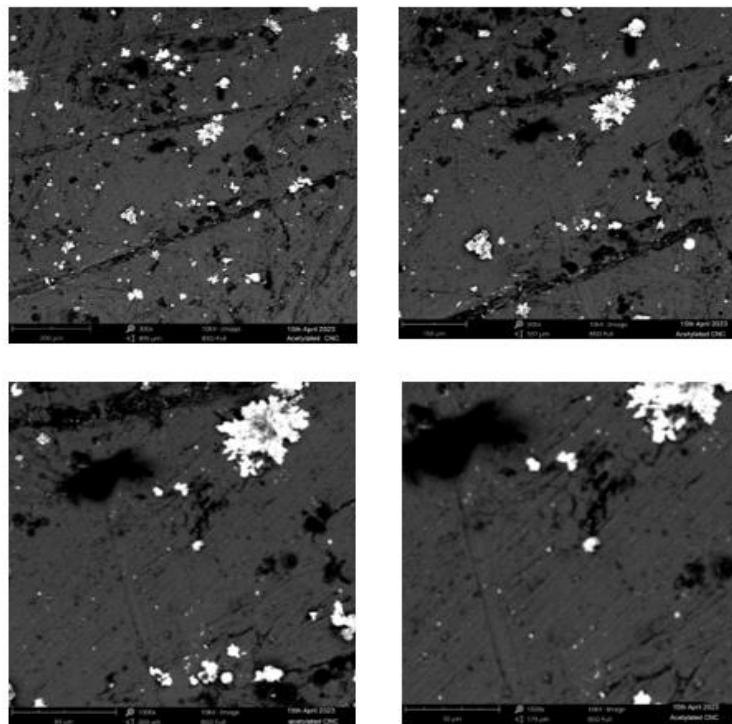


Fig. 3. SEM images of Cellulose triacetate

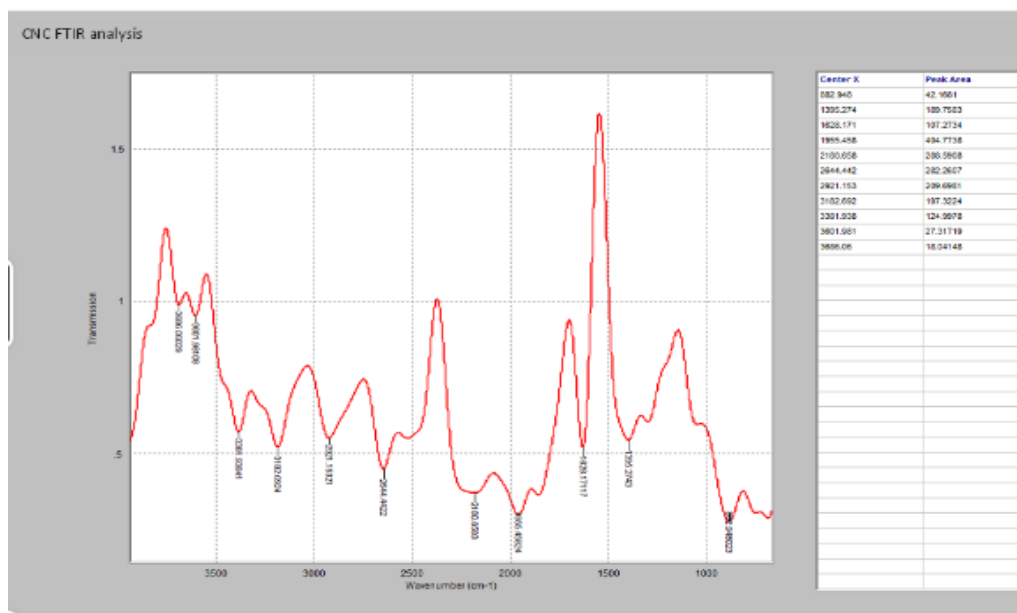


Fig. 4a. FTIR Spectra of CNCs

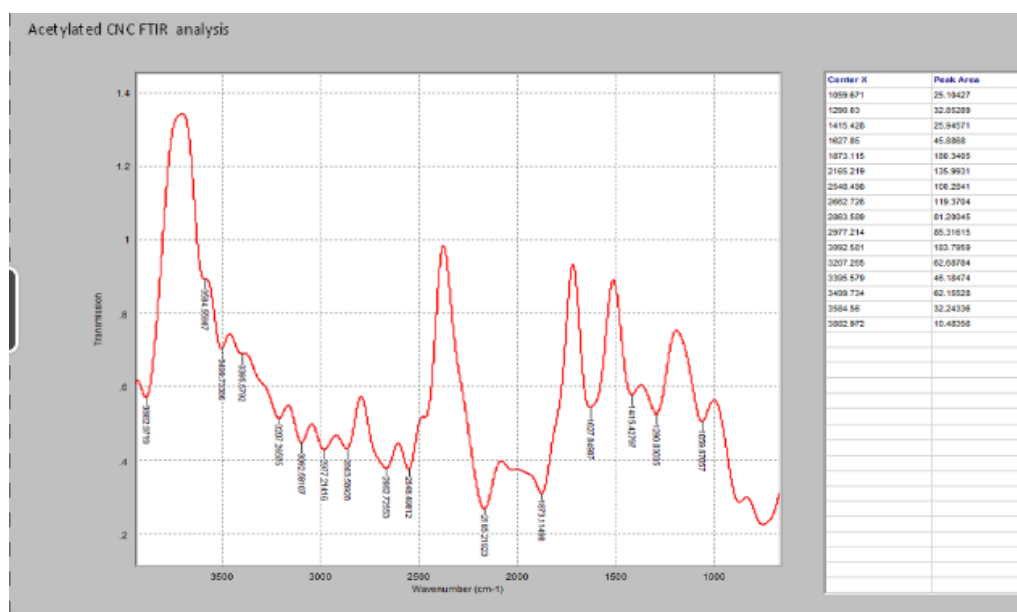
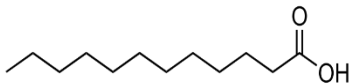
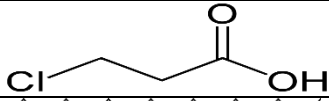
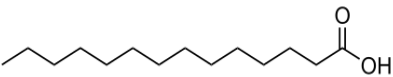
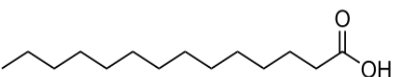
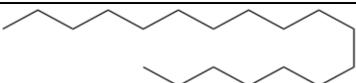
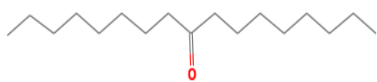
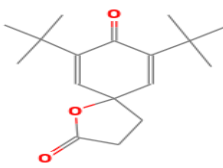
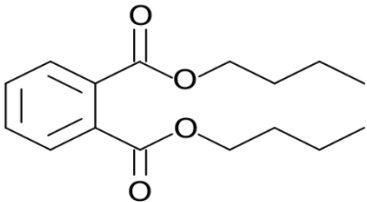
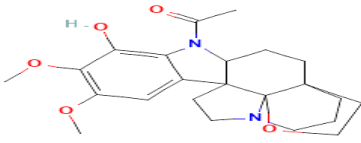
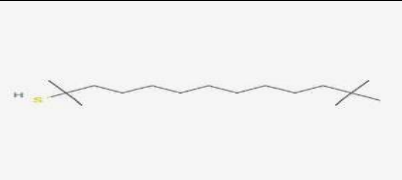
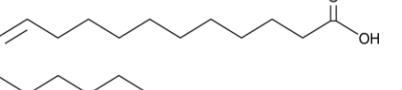
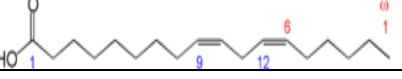
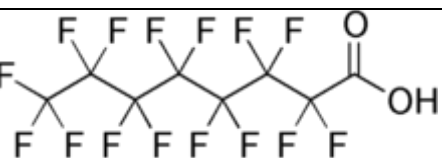
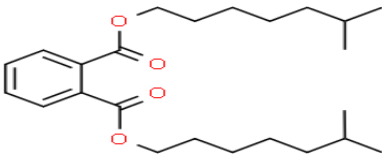
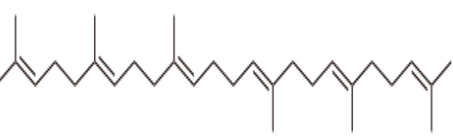


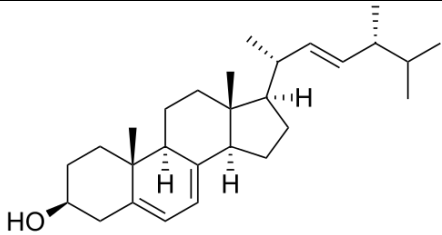
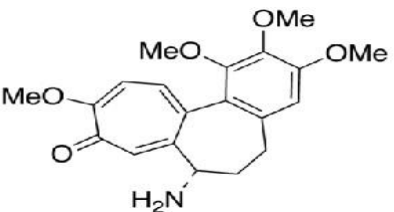
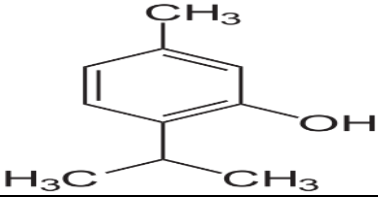
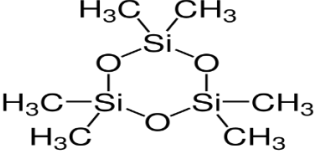
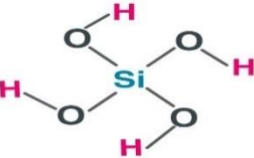
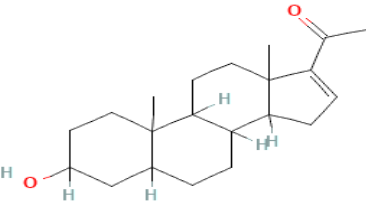
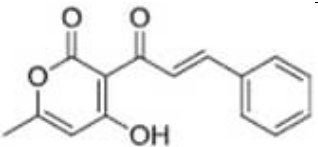
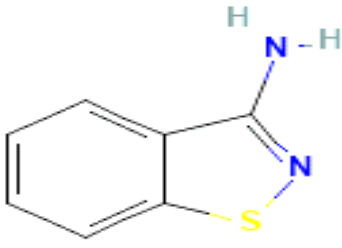
Fig. 4b. FTIR spectra of CTA

Table 6. GC-MS composition of CNCs

Peak	Reten- tion time	Compound name	Structure	% area
1	7.00	Tetradecane	<chem>CCCCCCCCCCCCCCCC</chem>	0.88
2	8.481	2,4-tert-butylphenol	<chem>CC(C)(C)c1cc(O)cc(C(C)(C)C)c1</chem>	0.46
3	8.611	Pentadecane	<chem>CCCCCCCCCCCCCCC</chem>	0.35

Peak	Reten- tion time	Compound name	Structure	% area
4	9.592	Dodecanoic acid		1.87
5	10.022	3-chloropropionic acid		0.34
6	10.185	Hexadecane		1.11
7	11.706	Heptadecane		0.50
8	12.556	Tetradecanoic acid		5.07
9	12.742	Tetradecanoic acid		0.62
10	13.017	9-Eicosene		2.24
11	13.165	Octadecane		2.18
12	13.331	1-octadecanesulphonyl chloride		0.49
13	13.920	9-Heptadecanone		0.94
14	14.062	7,9-Di-tert-butyl-1-oxaspiro (4,5)deca-6,9-diene		0.65
15	14.559	Nonadecane		0.74
16	14.707	Dibutyl phthalate		2.03
17	15.106	Aspidospermidin-17-ol		0.47

Peak	Retention time	Compound name	Structure	% area
18	15.320	n-Hexadecanoic acid		23.43
19	15.504	n-Hexadecanoic acid		1.68
20	15.616	tert-Hexadecanethiol		1.70
21	15.764	1-Docosene		5.64
22	15.890	Heptadecane		1.14
23	17.367	9,12-Octadecadienoic acid		0.61
24	17.475	Cis-Vaccenic acid		4.15
25	17.621	9,12-Octadecadienoic acid		0.95
26	18.285	1-Docosene		0.87
27	20.604	Pentadecafluorooctanoic acid		0.47
28	21.780	Diisooctyl phthalate		0.72
29	22.752	17-pentatriacontene		0.16
30	24.856	Squalene		1.13

Peak	Retention time	Compound name	Structure	% area
31	27.785	Ergosterol		1.22
32	30.006	N-Acetoacetyl-deacetylcolchicine		1.52
33	30.417	Thymol		2.27
34	31.052	Cyclotrisiloxane		13.73
35	31.095	Silicic acid		1.82
36	31.288	16-pregnenolone		11.30
37	31.350	3-(3,4-dimethoxycinnamoyl)-4-hydroxy-6-methyl-2H-pyran-2-one		5.59
38	36.599	<u>1,2-Benzisothiazol-3-amine</u>		-1.04

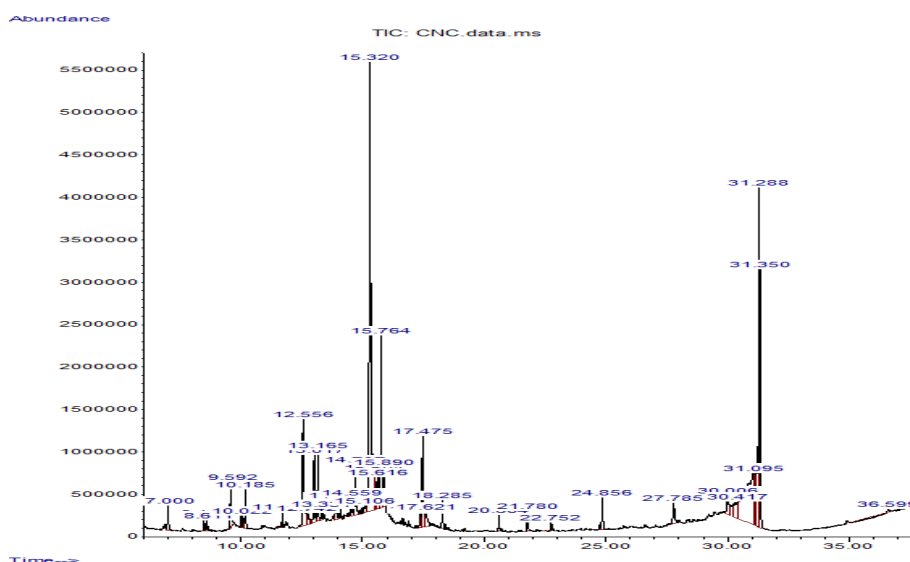


Fig. 5. GC-MS spectra for CNCs

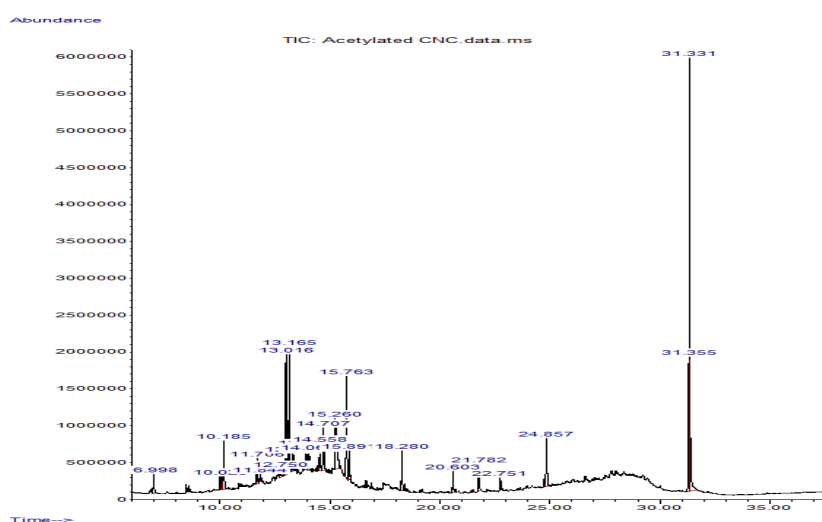


Fig. 6. GC-MS spectra of CTA

Table 7. GC-MS composition of CTA

Peak	Retention time	Compound name	Structure	% area
1	6.99	Tetradecane	<chem>CCCCCCCCCCCCCCCC</chem>	1.81
2	10.025	5-tetradecene	<chem>CCCCCCCC=CCCCCCCC</chem>	1.14
3	10.185	Hexadecane	<chem>CCCCCCCCCCCCCCCCCC</chem>	3.82
4	11.706	Heptadecane	<chem>CCCCCCCCCCCCCCCCC</chem>	1.86

Peak	Retention time	Compound name	Structure	% area
5	11.844	Dodecane		0.55
6	12.750	1-decanol		0.80
7	13.016	1-octadecene		9.76
8	13.165	10- methyl nonadecane		9.87
9	13.328	1-chloroeicosane		2.12
10	13.925	9-heptadecanone		2.95
11	14.060	Cetene		1.62
12	14.558	Teratetracontane		2.27
13	14.707	Didodecyl phthalate		4.62
14	15.260	n-Hexadecanoic acid		7.64
15	15.763	1-octadecene		8.01
16	15.891	Octadecane		1.96
17	18.280	1-Docosene		2.95
18	20.603	1-Docosene		1.68
19	21.782	Bis (2-ethylhexyl) phthalate		2.27
20	22.751	Pentadecafluorooctanoic acid		0.98

B

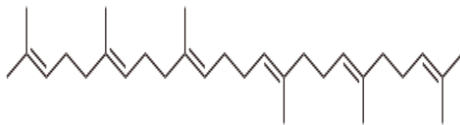
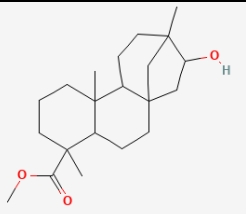
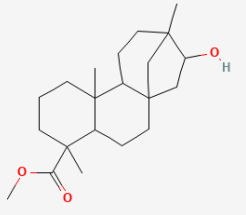
Peak	Retention time	Compound name	Structure	% area
21	Aq12wsezA FG	Squalene		4.73
22	31.331	Methyl dihydro isosteviol		15.39
23	31.355	Methyl dihydro isosteviol		11.19

Table 8. Weight Percent Gain (WPG) of acetylated cellulose

Run	Time (hours)	Conc. of H ₂ SO ₄ (wt%)	Temp (°C)	WPG (%)
1	2.50	5.50	47.50	72.22
2	4.00	1.00	35.00	64.44
3	1.00	10.00	60.00	29.87
4	0.02	5.50	47.50	65.63
5	5.02	5.50	47.50	46.05

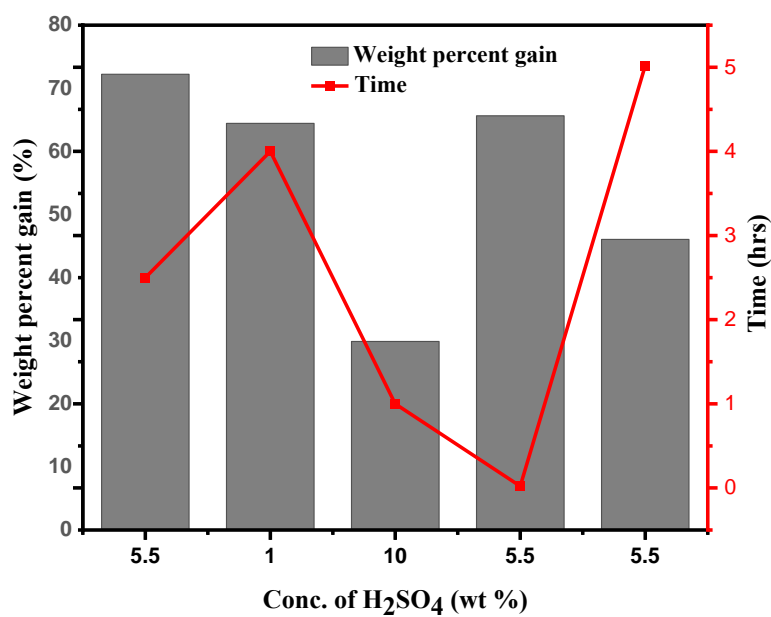


Fig. 7. Plot of WPG of acetylated cellulose as a function of catalyst concentration and reaction time

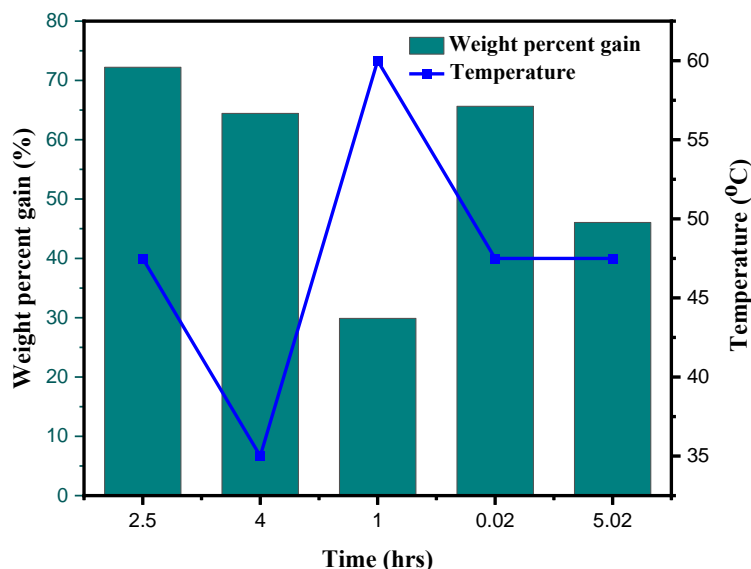


Fig. 8. Plot of WPG of acetylated cellulose as a function of temperature and reaction time

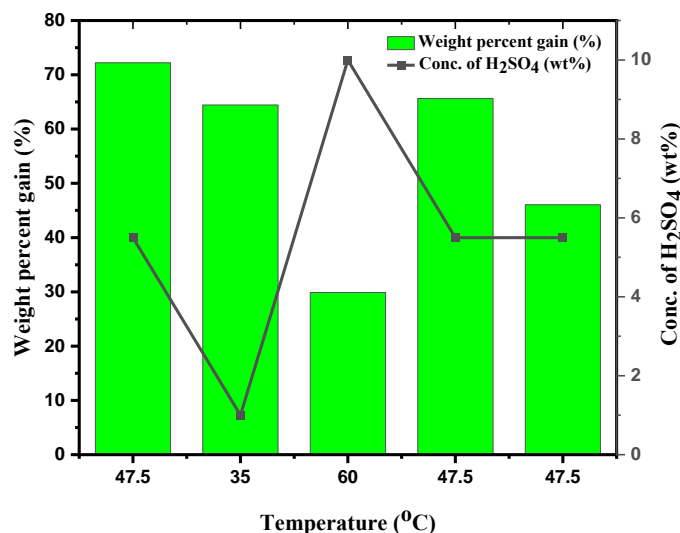


Fig. 9. A plot of WPG of acetylated cellulose as a function of temperature and catalyst concentration

4. CONCLUSION

In this investigation, CNCs were successfully extracted from bean seed hulls via sulphuric acid hydrolysis. Prior to this, the non-cellulosic components such as lignin, pectin, wax and hemicellulose were extensively removed by alkali treatment and bleaching. The chemical composition study reveals higher percentage of raw cellulose content with a lower percentage of lignin, hemicellulose and ash content. The reduced moisture content of CTA than that of CNCs means that CTA will make a better biofuel than CNCs. The percentage yield suggests that

large quantity of CNCs will be employed to obtain a greater yield of CTA. The solubility test showed that both the isolated CNCs and CTA were sparingly soluble in the polar solvent, water but insoluble in the organic solvent, ethanol. Some functional groups related to lignin and hemicellulose were identified using FTIR spectrometer implying that the pretreatment process did not remove all the lignin and hemicellulose from the isolated CNCs. The SEM analysis showed that the extracted CNCs has a magnified specific surface area and pore size than CTA making CNCs a better adsorbent than

CTA. Therefore, CNCs obtained from bean seed hulls have great potential to be utilized as adsorbent for heavy metals, crude oil, dyes, pesticides etc. as well as to be converted into CTA fabrics thereby remediating environmental pollution emanating from bean seed hulls. Further research such as the synthesis and characterization of organic nanoparticles of both CNCs and CTA, antimicrobial screening of the CNCs and CTA as well as the use of the synthesized organic nanoparticles of CNCs and CTA to adsorb heavy metals, crude oil, dyes and pesticides. In addition, the synthesized organic nanoparticles of CNCs and CTA should be subjected to Ultraviolet Visible Spectroscopy (UV-Vis), Fourier Transform Infrared Spectroscopy (FTIR), Gas Chromatography-Mass Spectrometry (GC-MS) and Nuclear Magnetic Resonance Spectroscopy (NMR) analyses so as to elucidate their structures and formulae.

ACKNOWLEDGEMENTS

The authors are very grateful to Docchy's Analytical Laboratory and Environmental Services, Awka Anambra State and Department of Chemical Engineering, Ahmadu Bello University, Zaria Kaduna State, Nigeria for providing the necessary facilities for carrying out the study.

COMPETING INTERESTS

The authors declare that no competing interest existed among them as regards to finance, contributions to paper writing and position of authors in this article.

REFERENCES

1. Nsude OP, Orié KJ. Thermodynamic and adsorption analysis of corrosion inhibition of mild steel in 0.5M HCl medium via ethanol extracts of *Phyllanthus mellerianus*. *American Journal of Applied Chemistry*. 2022;10(3):67-75.
2. Auffhaminer M, Ramanathan V, Vincent J. *Proceedings of the National Academy of Science*. 2006;5(52):19668-19672.
3. Agarwal B. Gender and forest conservation: The impact of women's participation in community forest governance. *Ecological Economics*. 2009;68(11):2785-2799.
4. Nwajioji CC, Otaigbe J, Oriji O. Isolation and characterization of microcrystalline cellulose from papaya stem. *Der Pharma Chemica*. 2019;11(3):19-26.
5. Nsude OP, Orié KJ, Udezo PI, Ogbobe O, Chime CC. Isolation, physicochemical and BET analysis of cellulose from *Pentaclethra macrophylla* benth (oil bean). *Pod Biomass Wastes International Research Journal of Pure and Applied Chemistry*. 2022;23(5):9-22. DOI:10.9734/IRJPAC/2022/v23i530474.
6. Aridi AS, Yusuf YA, Nyuk LC, Ishak NA, Mohammad Yusuf YNN. Isolation of cellulose from *Leucaena leucocephala* mature pods and how different bleaching agents affect its characterization. *Materials Performance and Characterization*. 2022;11(1):236-243.
7. Onuegbu TC. Improving fuel wood efficiency in rural Nigeria: Briquette technology chemistry in Nigeria. *A National Magazine in the Chemical Society of Nigeria*. 2010;4(3):35-39.
8. Saha BC. Hemicellulose bioconversion. *Journal of Industrial Microbiology and Biotechnology*. 2003;30:279-291.
9. Candido RG, Godoy GG, Goncalves AR. Study on sugarcane bagasse pretreatment with sulphuric acid as a step of obtaining cellulose. *WASET*. 2012;61:101-105.
10. Bello A, Isa MT, Aderemi BO, Mukhtar B. Acetylation of cotton stalk for cellulose acetate production. *American Scientific Research Journal for Engineering, Technology and Sciences (ASRJETS)*. 2016;15(1):137-150.
11. Malladi R, Nagalakshmaiah M, Robert M, Elkoun S. Importance of agricultural and industrial waste in the field of nanocellulose and recent industrial developments of wood based nanocellulose: A review. *ACS Sustainable Chemistry & Engineering*. 2018;1-70. DOI:10.1021/acssuschemeng.7b03437
12. Klemm D, Kramer F, Moritz S, Lindstrom T, Ankerfors M, Gray D, Dorris A. Nanocelluloses: A new family of nature-based materials. *Angew. Chem. Int. Ed*. 2011;50(24):5438-5466. DOI:10.1002/anie.201001273
13. Finar IL. Organic chemistry: Stereochemistry and the chemistry of natural products. Vol 2, 5th Edition. Pearson Education Limited. 2014;350-353.
14. De Souza Lima MM, Borsali RR. Cellulose microcrystals: Structure, properties and applications. *Macromol. Rapid Commun*. 2004;25(7):771-789.

- DOI: 10.1002/marc.200300268
15. Sheltami RM, Abdullah T, Ahmad I, Dufresne A, Kargarzadeh H. Extraction of cellulose nanocrystals from mengkuang leaves (*Pananus tectorius*). Carbohydrate Polymers. 2012;88(2):772-779. Available: <https://doi.org/10.1016/j.carbpol.2012.01.062>
 16. Habibi Y, Lucia L, Rojas O. Cellulose nanocrystals: Chemistry self-assembling and applications chemical reviews. 2010;110(6):3479-3500. DOI:10.1021/cr900339w
 17. He X, Luzi F, Yang W, Xiao Z, Torre L, Xie Y, Puglia D. Citric acid as green modifier for tuned hydrophilicity of surface modified cellulose and lignin nanoparticles. ACS Sustainable Chemistry and Engineering. 2018;6(8):9966-9978. Available: <https://doi.org/10.1021/acssuschemeng.8b01202>.
 18. Plackett D, Sodergard A. Natural fibres, biopolymers and biocomposites. CRC Press, Boca Raton. 2005;569.
 19. Yang W, Fortunate E, Luzi F, Kenny JM, Torre L, Puglia D. Lignocellulosic /based bionanocomposites for different industrial applications. Current Organic Chemistry. 2018;22(12):1205-1221. Available: <https://doi.org/10.2174/1385272822666180515120948>
 20. Morrison RT, Boyd RN, Bhattacharjee SK. Organic chemistry. 8th Edition, Dorling Kindersley (India) Pvt. Ltd. 2018;1267:1274-1276.
 21. Lamaming J, Hashim R, Leh CP, Sulaiman O, Sugimoto T, Nasir M. Isolation and characterization of cellulose nanocrystals from parenchyma and vascular bundle of oil palm trunk (*Elaeis guineensis*). Carbohydrate Polymers. 2012;88(2):772-779.
 22. Luzi F, Puglia D, Sarasini F, Tirillo J, Maffei G, Zuorro A, Lavecchia R, Kenny JM, Torre L. Volarization and extraction of cellulose nanocystals from North African grass: *Ampelodesmos mauritanicus* (DISS). Carbohydrate Polymers. 2019;209:328-337. Available: <https://doi.org/10.1016/j.carbpol.2019.01.048>
 23. Sacui IA, Nieuwendaal RC, Burnett DJ, Stranick SJ, Jorfi M, Weder C, Johan FE, Olsson RT, Gilman JW. Comparison of the properties of cellulose nanocrystals and cellulose nanofibrils isolated from bacteria, tunicate and wood processed using acid, enzymatic, mechanical and oxidative methods. ACS Applied Materials and Interfaces. 2014;6(9):6127- 6138. Available: <https://doi.org/10.1021/am500359f>
 24. Matos RM, Cavaille JY, Dufresne A, Gerard JF, Graillat C. Processing and characterization of new thermoset nanocomposites based on cellulose whiskers. Composite Interfaces. 2000;7(2):117-131. Available: <https://doi.org/10.1163/156855400300184271>
 25. Neus Anglés M, Dufresne A. Platicized starch/ tunicin whiskers, nanocomposite materials.2. Mechanical Behaviours. Macromolecules. 2001;34(9):2921-2931. Available: <https://doi.org/10.1021/MA001555H>
 26. simple.m.wikipedia.org > wiki > File: Cellulose triacetate structure.jpg. Retrieved on Sunday 14 January 2024, 11:59 am WAT.
 27. Akpuaka MU. Essentials of natural products chemistry. 1st Edition. Mason Publishers Enugu, Nigeria. 2009;25-30.
 28. www.vedantu.com>chemisy>us... Retrieved on the 1st of August 2023 at 03:20am West Central African Time.
 29. Badea GI, Radu GL. Introductory chapter: Carboxylic acids-keyrole in life sciences; 2018. Available: <https://dx.doi.org/10.5772/intechopen.77021>
 30. Kalgutkar AS, Daniels JS. Carboxylic acids and their bioisosteres. In: Metabolism, pharmacokinetics and toxicity of functional groups: Impact of the building blocks of medicinal chemistry on ADMET. London: Royal Society of Chemistry. 2010;99-167.
 31. Pfaff AR, Beltz J, King E, Ercal N. Medicinal thiols: Current status and new perspectives Mini Rev. Med. Chem. 2020;20(6):513-529. DOI:10.2174/1389557519666191119144100
 32. Smith A. Nova Biomedical: The importance of ketones from a clinical and medical perspective. News-Medical; 2023. Available:<https://www.newsmedical.net/news/20230308/The-importance-of-ketones->

- from-a-clinical-and-medical-perspective.aspx>.
33. Carter A, Jewel T. What are the medical and health uses of phenol? An overview. Healthcare; 2019.
 34. Al Mamari HH. Phenolic compounds: Classification, chemistry and updated techniques of analysis and synthesis. Chapter metrics overview. Open access peer-reviewed chapter. Healthline media; 2021. DOI:10.5772/intechopen-98958.
 35. Haminiuk CW, Maciel GM, Plata-Oviedo MSV, Peralta RM. Phenolic compounds in fruits- an overview. Food Sci. Technol. Int. 2012;47:2022-2044. Available: <https://doi.org/10.1111/j.13652621.2012.03067.x>
 36. Das S, Das J, Samadder A, Khuda-Bukhsh AR. Dihydroxy –isosteviol methyl ester from *pulsatilla nigricans* induces apoptosis in Hela cells: Its cytotoxicity and interaction with calf thymus DNA. Phototherapy Research. 2012;27(5):664-673. Available: <https://doi.org/10.1002/ptr.4768>
 37. Wang Y, Qian H. Phthalates and their impacts on human health. Healthcare. 2021;9(5):603. DOI:1.3390/healthcare9050603
 38. Ericson-Neilsen W, Kaye AD. Steroids: Pharmacology, complications and practice delivery issues. The Ochsner Journal. 2014;14(2):203-207.
 39. Sharma S, Anand N. Approaches to design and synthesis of antiparasitic drugs. Pharmacochimistry Library. 1997;25:296-324. Available: [https://doi.org/10.1016/S0165-7208\(97\)80034-7](https://doi.org/10.1016/S0165-7208(97)80034-7)
 40. Negi BYS. Studies on cellulose nanocrystals isolated from groundnut shells. Carbohydrate Polymers. 2017;157:1041-1049.
 41. Carreón T, Herrick RL. Aliphatic hydrocarbons. Wiley Online Library; 2012. Available:<https://doi.org/10.1002/0471435139.tox049.pub2>
 42. www.google.com. Retrieved on the 1st of August 2023 at 2:30am West Central African Time
 43. Dumonteil G, Berteina-Rabolo S. Synthesis of conjugated dienes in natural compounds. Journals Catalysts. 2022;12(1):86. DOI.org/10.3390/catal12010086
 44. Rani A, Jain S, Kumar R, Kumar A. 1,5-Bis (2-hydroxyphenyl) pent-1,4-diene-3-one: A lead compound for the development of broad-spectrum anti-bacterial agents. S. Afr. J. Chem. 2010;63:31-35. Available: <https://journals.sabinet.co.za/sajchem/>
 45. Xiao Y, Liu Y, Wang X, Li M, Lei H, Xu H. Cellulose nanocrystals prepared from wheat bran: Characterization and cytotoxicity assessment. International Journal of Biological Macromolecules. 2019;140:225-233.
 46. Kassab Z, Abdellaoui Y, Salim MH, El Achaby M. Cellulosic Materials from *Pealpisum sativum* and broad beans (*vicia faba*) pods agro-industrial residues. Material Letters. 2022;280:128539. Available:<https://doi.org/10.1016/j.matlet.2020.128539>
 47. Furniss BS, Hannaford AJ, Smith PWG, Tatchell AR. Vogel's textbook of practical organic chemistry. 5th Edition. Pearson Education limited, England. 1196-1204, 1225, 1289-1398.
 48. ASTM International. ASTM D792-17 Standard test methods for density, specific gravity (Relative Density of plastics by displacement), cellulose, lignin, hemicellulose, moisture content and melting point. West Conshohocken, PA: ASTM International; 2017.
 49. American Oil Chemists' Society (AOAC). Official methods and recommended practices of the AOCS (7th ed.). AOCS Press; 2017.
 50. ASTM International. ASTM E70-18 Standard Test for pH of aqueous solutions with the glass electrode. West Conshohocken, PA: ASTM International; 2015.
 51. www.quora.com. Retrieved from Google scholar on Tuesday, 9 January, 2024 at 3:48am WAT.
 52. Azogu CI, Laboratory Organic Chemistry: Techniques, qualitative analysis, organic preparations and spectroscopy. 2nd Edition. Maybinson Book Publishers, New Jersey, USA. 2010;153-200.
 53. Ajayi IA, Oderinde RA, Kajogbola DO, Uponi JI. Oil content and fatty acid composition of some underutilized legumes from Nigeria. Journal of Food Chemistry. 2006;99:115-120. DOI:10.1016/j.foodchem.2005.06.045.
 54. Ibourki M, Azouguigh F, Jadouali S, Saka E, Bijla L, Majourhat K, Gharby S, Lakniffi

- A. Physical fruit traits, nutritional composition and seed oil fatty acid profiling in the main date palm (*Phoenix dactylifera L.*) varieties grown in Morocco. Hindawi Journal of Food Quality. Article ID5138043, 2021;12.
Available:<https://doi.org/10.1155/2021/5138043>.
55. Alkinjokun A, Petrik LF, Ogunfowokan J, Ajao J, Ojumu TV. Isolation and characterization of nanocrystalline cellulose from cocoa pod husk (CPH) biomass wastes. Heliyon. 2021;7(4):e06680.
56. Alhaji MH, Oparah EN, Yakubu MK, Maju CC, Suleiman H, Akawu I, Musa TAD, Aliyu S. Production, properties and applications of cellulose/waste leather buff composite (WLB) for environmental sustainability and recyclability. Journal of Chemical Society of Nigeria. 2021;46(3):610-617.
Available:
<https://doi.org/10.46602/jcsn.v46i3.634>
57. Danbature WL, Shehu Z, Joshua J, Adam MM. Moringa oleifera root-mediated synthesis of nanosilver particles and the antibacterial applications. Journal of Chemical Society of Nigeria. 2021;46(3): 504-516.
Available:<https://doi.org/10.46602/jcsn.v446i3.626>
58. Ekeoma MO, Okoye PAC, Ajiwe VIE, Hameed BH. Modified coconut shell as active heterogeneous catalyst for the transesterification of waste cooking oil. J. Chem. Soc. Nigeria. 2020;45(2): 360-368.
59. Pam AA, Adeyi AA, Obiyenwa GK, Yinusa I, Salawu OW. Adsorption of methylene blue from aqueous solution using iminodiacetic acid supported montmorillonite adsorbent. J. Chem. Soc. Nigeria. 2020;45(2):288-297.
60. Saravanan R, Ravikumar I. The use of new chemically modified cellulose for heavy metal ion adsorption and antimicrobial activities. Journal of Water Resources and Protection. 2015;7:530-545.
61. Williams DH, Fleming I. Spectroscopic methods in organic chemistry. 3rd Edition. McGraw-Hill Book Company (UK) Limited England, 1980;47-73.
62. Flauzino NWP, Silverio HA, Dantas NO, Pasquini D. Extraction and characterization of cellulose nanocrystals from agro-industrial residue-soy hulls, Ind. Crop Prod. 2013;42:480-488.
63. George J, SN S. Cellulose nanocrystals: Synthesis, functional properties and applications. Nanotechnology Sci. Appl; 2015.
DOI: 10.2147/NSA.S64386

© 2023 Morah et al.; This is an Open Access article distributed under the terms of the Creative Commons Attribution License (<http://creativecommons.org/licenses/by/4.0>), which permits unrestricted use, distribution, and reproduction in any medium, provided the original work is properly cited.

Peer-review history:

The peer review history for this paper can be accessed here:
<https://www.sdiarticle5.com/review-history/111542>